Ordu Üniversitesi Bilim ve Teknoloji Dergisi
Ordu Üniv. Bil. Tek. Derg.

Ordu University Journal of Science and Technology
Ordu Univ. J. Sci. Tech.

E-ISSN: 2146-6459 2025, 15(2), 339-351 Araştırma Makalesi / Research Article
http://doi.org/10.54370/ordubtd.1771474

New Isatin Derivatives Based Isopropyl-Thiosemicarbazone: Synthesis, Spectroscopic Characterization, and Theoretical Studies

Hasan Yakan[1]

[1]Ondokuz Mayıs University, Faculty of Education, Department of Chemistry Education, Samsun, Türkiye

Geliş Tarihi / Received Date: 24.08.2025 Kabul Tarihi / Accepted Date: 20.11.2025

Abstract

A series of isatin derivatives based isopropyl-thiosemicarbazone (4–11) were synthesized through the reaction of various isatin derivatives with *N*-isopropylhydrazinecarbothioamide. The thiosemicarbazide intermediate was obtained by reacting isopropyl isothiocyanate with hydrazine monohydrate. Structural characterization and purity assessment of the synthesized compounds were performed using ^{1}H and ^{13}C NMR, FT-IR spectroscopy, and elemental analysis. Furthermore, to shed light on the stability and reactivity of the compounds, DFT calculations were performed, and the results were used to comparatively analyse the structural and electronic characterization of the compounds.

Keywords: isatin, thiosemicarbazone, spectroscopic techniques, DFT calculations

İzopropil-Tiyosemikarbazon Bazlı Yeni İzatin Türevleri: Sentez, Spektroskopik Karakterizasyon ve Teorik Çalışmalar

Öz

İzopropil-tiyosemikarbazon (4–11) bazlı bir dizi izatin türevi, çeşitli izatin türevlerinin *N*-izopropilhidrazinkarbotiyoamid ile reaksiyonu yoluyla sentezlendi. Tiyosemikarbazit ara ürünü, izopropil izotiyosiyanatın hidrazin monohidrat ile reaksiyona sokulmasıyla elde edildi. Sentezlenen bileşiklerin yapısal karakterizasyonu ve saflık değerlendirmesi, ^{1}H ve ^{13}C NMR, FT-IR spektroskopisi ve elementel analiz kullanılarak gerçekleştirildi. Ayrıca, bileşiklerin kararlılığı ve reaktivitesini aydınlatmak için DFT hesaplamaları yapıldı ve sonuçlar, bileşiklerin yapısal ve elektronik karakterizasyonunu karşılaştırmalı olarak analiz etmek için kullanıldı.

Anahtar Kelimeler: izatin, tiyosemikarbazon, spektroskopik teknikler, DFT hesaplamaları

Sorumlu Yazar / Corresponding Author: Hasan Yakan hasany@omu.edu.tr

Introduction

Thiosemicarbazones represent a significant class of organosulfur compounds in synthetic organic chemistry, distinguished by the presence of the –NH–C(=S)NH–N= functional group. Their structural versatility and high reactivity make them useful intermediates in the synthesis of a wide range of biologically active molecules. The structural versatility and functional tunability of thiosemicarbazones have made them important scaffolds in the design of new pharmacologically active agents. They serve as key intermediates in the synthesis of heterocyclic compounds and metal complexes, and have been widely explored for their broad spectrum of biological activities, including antitubercular (Ozcan et al., 2023), anticonvulsant (Deng & Song, 2014; Kshirsagar et al., 2009), urease inhibitor (Hameed et al., 2015; Islam et al., 2019; Shehzad et al., 2020), antiviral (Sevinçli et al., 2020), anticancer (Czylkowska et al., 2024; Shakya & Yadav, 2020), antioxidant (Çavuş, 2025; Hernández et al., 2023), antimicrobial (Gündüz et al., 2021), and antibacterial (Govender et al., 2019) properties. There has been a growing interest in Schiff base-derived thiosemicarbazones in recent years, driven by their potential in various in vitro and in vivo biological investigations. They have exhibited substantial antibacterial and antifungal (Pervez et al., 2008), antimicrobial (Al-Amiery et al., 2012), antioxidant (Muğlu, 2020), anti-inflammatory (Subhashree et al., 2017), anti-HIV (Bal et al., 2005), anticancer (Arafath, 2024; Tokalı, 2023b), ameliorative effect (Karakuş et al., 2024), and enzyme inhibitor (Tokalı et al., 2021) activities.

Density Functional Theory (DFT) is a widely used quantum chemical computational method that allows for the accurate prediction of the molecular geometry, electronic structure, and physicochemical properties of organic and inorganic compounds. By focusing on the electron density rather than the many-body wavefunction, DFT provides an efficient yet reliable framework for exploring electronic behaviors and structure–property relationships in complex molecular systems (Kohn et al., 1996; Parr & Yang, 1984; Parr, 1989). In recent years, DFT has become an essential tool in the field of computational chemistry, particularly for modeling biologically active heterocycles and drug-like molecules. It enables the calculation of frontier molecular orbitals (HOMO–LUMO), energy gaps, dipole moments, molecular electrostatic potentials (MEP), and global reactivity descriptors, which are crucial for understanding chemical reactivity, stability, and potential biological activity (Cramer, 2013; Koch & Holthausen, 2015).

In the present study, a new series of isatin-based isopropyl-thiosemicarbazone derivatives (4–11) were synthesized via the condensation reaction of various isatin derivatives with *N*-isopropylhydrazinecarbothioamide under mild conditions. The structures of the synthesized compounds were confirmed through a combination of spectroscopic techniques, including Fourier-transform infrared spectroscopy (FT-IR), proton and carbon nuclear magnetic resonance spectroscopy (^{1}H NMR and ^{13}C NMR), and elemental (CHNS) analysis. These characterization methods provided clear evidence for the successful formation of the targeted thiosemicarbazone compounds and allowed for the identification of key functional groups and structural features.

Furthermore, to gain deeper insight into the structural, electronic, and reactive properties of the synthesized molecules, quantum chemical calculations were performed using density functional theory (DFT) at the B3LYP/6-311++G(d,p) level of theory. Theoretical parameters such as frontier molecular orbitals (HOMO–LUMO energies), energy gaps, dipole moments, and molecular electrostatic potential (ESP) maps were calculated to evaluate the electronic properties, chemical reactivity, and stability of the compounds. The DFT results were also used to support the experimental findings and to explore the influence of various substituents on the electronic behavior of the molecules.

Materials and Methods

Materials and Instrumentals

All chemicals were purchased from Merck, Sigma, or Aldrich Chemical Company and used without any further purification. Spectroscopic-grade solvents were utilized throughout the study. Elemental analyses were carried out using a Eurovector EA3000-Single analyzer. Melting points were measured with a Stuart SMP30 apparatus and are reported without correction. FT-IR spectra were obtained using a Bruker Alpha spectrometer. ^{1}H and ^{13}C NMR spectra were recorded on a Bruker Avance DPX-400 MHz spectrometer, with DMSO-d_6 as the solvent. UV–Vis absorption spectra were measured using a Shimadzu Pharmaspec 1700 spectrophotometer. NMR signal multiplicities are indicated as follows: s = singlet, d = doublet, dd = doublet of doublets, t = triplet, and m = multiplet

Synthesis Procedure

Isopropyl isothiocyanate (8.00 mmol) was added dropwise to a solution of hydrazine monohydrate (8.00 mmol) in 20 mL of ethanol under vigorous stirring, while maintaining the temperature in an ice bath. To ensure the reaction proceeded to completion, the mixture was refrigerated overnight. The formed thiosemicarbazide intermediate was subsequently separated by filtration, then dried and recrystallized using ethanol. After then, a solution containing *N*-isopropylhydrazinecarbothioamide (4.00 mmol) and isatin derivatives (4.00 mmol) in 20 mL of aqueous ethanol was treated with a few drops of hydrochloric acid. The reaction mixture was heated under reflux at 78 °C for 3–5 hours. Upon completion, the resulting solid was collected by filtration, rinsed with cold ethanol, and allowed to air dry. The targeted products were successfully synthesized in good yields (60–95%), as illustrated in Figure 1. The synthesis was carried out using a modified version of previously reported procedures (Yakan, 2020; Zhang et al., 2007). The synthesis of compound 4 was previously known in the literature (Hall et al., 2011). Compounds 5, 7 and 11 are known commercially, but their synthesis is unknown.

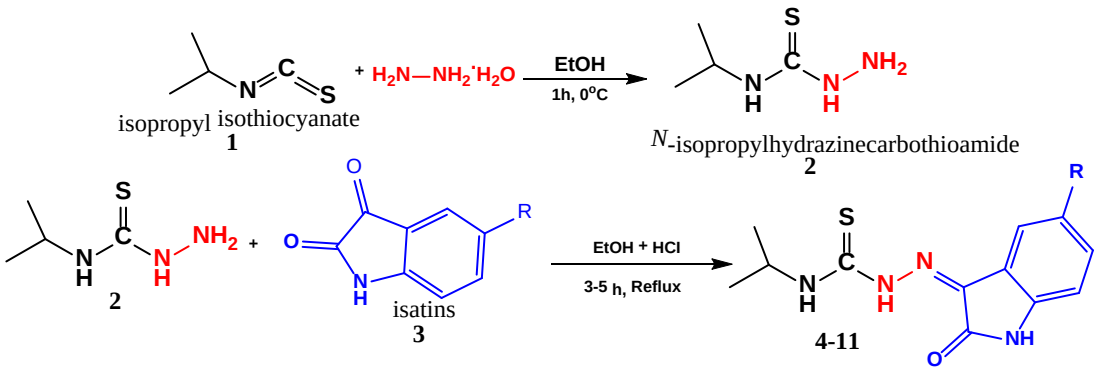

Figure 1. Synthesis Pathway of New Isatin Based Thiosemicarbazones (4–11)

Calculation Process

The calculations were performed within the framework of density functional theory (DFT) (Hohenberg & Kohn, 1964; Kohn & Sham, 1965) using the ORCA program (Neese, 2022). The employed method is the B3LYP functional, which combines Becke's three-parameter exchange functional with the correlation functional developed by Lee, Yang, and Parr. The 6-311++G(2d,2p) basis set along with the D4 dispersion correction was chosen for the computations. Additionally, TightSCF and TightOpt convergence criteria were applied to achieve higher accuracy, and auxiliary basis sets were automatically determined using the Autoaux option. No constraints related to molecular symmetry were imposed during the process, thus preserving the natural geometries of the systems. The absence of any imaginary frequencies in the IR frequency analyses following geometry

optimizations indicates that the obtained structures correspond to true minima on the potential energy surface.

For the evaluation of electronic properties, gas-phase analyses were conducted at the same level of theory. In this context, the energy levels of frontier molecular orbitals were determined, and from these data, global reactivity descriptors such as chemical hardness, electronegativity, and electrophilicity were calculated. This allowed for significant insights into the reactivity and thermodynamic stability of the molecules.

In accordance with the experimental procedure, new geometry optimizations were performed under DMSO solvent conditions using the CPCM-SCRF approach to investigate the behavior of the compounds in solution for NMR calculations. The computed NMR chemical shifts were referenced to the TMS compound; absolute shielding constants for TMS (31.805 ppm for ^{1}H and 183.726 ppm for ^{13}C) obtained at the B3LYP/6-311++G(2d,2p) level were used to determine these values.

Results and Discussion

Physical Properties

The current experimental results for the physicochemical data, melting points, yields, and elemental analyses are given in Tables 1 and 2.

Tablo 1. The Physical Data for the Synthesized Compounds

Compounds	Melting Point (°C)	Yields (%)	Colour
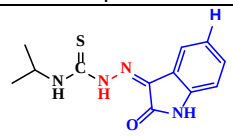	246-247	60	Yellow
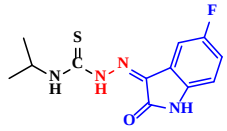	240-241	69	Light Brown
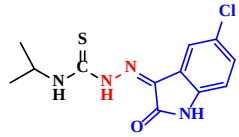	249-250	95	Light Orange
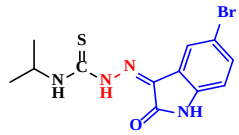	246-247	81	Light Orange
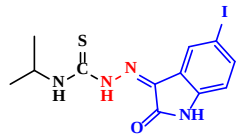	269-270	74	Yellow
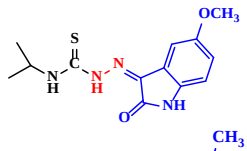	216-217	75	Red
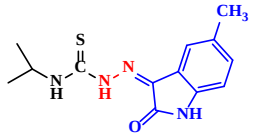	253-254	73	Orange
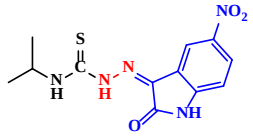	263-264	79	Yellow

Table 2. Elemental Analysis Results of the Compounds

			Calculated			Experimental		
Comp.	Mol. Formula	M.W.(g/mol)	C%	H%	N%	C%	H%	N%
4	$C_{12}H_{14}N_4OS$	262.33	54.94	5.38	21.36	54.90	5.39	21.38
5	$C_{12}H_{13}FN_4OS$	280.32	51.42	4.67	19.99	51.45	4.66	20.02
6	$C_{12}H_{13}ClN_4OS$	296.78	48.56	4.42	18.88	49.01	4.41	18.86
7	$C_{12}H_{13}BrN_4OS$	341.23	42.24	3.84	16.42	42.22	3.83	16.45
8	$C_{12}H_{13}IN_4OS$	388.23	37.12	3.38	14.43	37.10	3.38	14.46
9	$C_{13}H_{16}N_4O_2S$	292.36	53.41	5.52	19.16	53.45	5.51	19.14
10	$C_{13}H_{16}N_4OS$	276.36	56.50	5.84	20.27	56.53	5.82	20.24
11	$C_{12}H_{13}N_5O_3S$	307.33	46.90	4.26	22.79	46.86	4.26	22.77

IR Spectral Analysis

Considering the FT-IR spectra of the compounds, the asymmetric and symmetric stretching frequencies of the amino group (–NH_2) as a characteristic doublet peak were not observed at 3400 – 3300 cm^{-1}. Instead, a novel imine group (CH=N) vibration was observed at 1528 – 1505 cm^{-1}.

This evidence confirmed the expected successful reaction (see at Figures S1-S8 in Supplementary information). For all compounds (4-11), a amine group (-NH) vibration of isatin ring were detected in the range 3396 – 3312 cm^{-1}, while the amine group (-NH) vibration of the thiosemicarbazone moiety were observed at 3220 – 3165 cm^{-1}.

Table 3. Experimental and Theoretical IR Vibration Frequencies of the Synthesized Compounds (cm^{-1})

	Comp.	υ_{NH} (ist)	υ_{NH} (tsc)	υ_{C-H} (Aromatic)	υ_{C-H} (Aliphatic)	$\upsilon_{C=O}$	$\upsilon_{C=N}$	$\upsilon_{C=S}$	υ_{C-N} istC-N N-CH N-C=S	Specific Vib.
Experimental	4	3338	3173	3068	2876	1682	1519	1363	1191 1137 996	-
	5	3349	3173	3073	2884	1684	1516	1366	1183 1155 1133	C-F:1111
	6	3366	3169	3072	2929	1685	1508	1346	1136 1110 1059	C-Cl:1059
	7	3351	3168	3050	2929	1687	1505	1301	1183 1150 1108	C-Br:753
	8	3358	3168	3075	2826	1689	1521	1305	1185 1136 1118	C-I:566
	9	3364	3165	3027	2829	1685	1517	1341	1187 1136 1115	C-O:1023
	10	3312	3220	3016	2873	1699	1528	1301	1196 1159 1123	-
	11	3396	3194	2978	2869	1706	1518	1332	1194 1145 1119	NO_2:1462, 1293

Calculated	4	3646.76	3565.40 3438.14	3202.06- 3175.83	3115.84- 3025.73	1750.16	1612.85	1422.28	1278.24 1198.82 1160.54	-
	5	3648.52	3566.73 3433.38	3213.31- 3190.24	3116.25- 3026.32	1750.06	1610.02	1423.91	1285.68 1201.33 1156.43	C-F: 1170.40
	6	3646.83	3566.24 3435.81	3216.30- 3189.81	3115.90- 3026.47	1751.17	1609.59	1420.82	1274.21 1198.01 1159.11	C-Cl: 1085.55
	7	3646.65	3566.37 3435.46	3217.63- 3189.97	3115.82- 3026.61	1751.24	1608.92	1420.70	1274.32 1197.84 1159.08	C-Br: 887.85
	8	3646.63	3558.92 3442.23	3210.79- 3187.01	3111.26- 3026.51	1751.08	1609.67	1418.07	1274.43 1192.30 1152.61	C-I: 686.42
	9	3650.61	3566.16 3435.99	3222.30- 3185.04	3116.71- 3024.81	1746.93	1613.27	1418.59	1294.87 1200.28 1160.36	C-O: 1056.12
	10	3647.65	3564.33 3439.45	3189.74- 3172.05	3115.76- 3025.38	1748.60	1614.50	1419.11	1286.79 1199.51 1157.66	-
	11	3640.59	3566.01 3442.09	3236.20- 3195.31	3116.12- 3027.90	1756.95	1607.74	1431.79	1307.06 1196.54 1156.14	NO_2: 1360.49, 1096.74

The aromatic proton vibrations were observed in the range 3073 – 2978 cm^{-1}, aliphatic proton vibrations were observed in the range 2929 – 2826 cm^{-1}, the characteristic –C=O vibration of the isatin ring were observed at 1706 – 1682 cm^{-1}, the –C=S signals of the thiosemicarbazone moiety were observed at 1366 – 1301 cm^{-1}, the –C–N group vibrations were observed at 1196 – 996 cm^{-1}. For the compounds 5-8, the –C–F, –C–Cl, –C–Br, and –C–I vibration signals were observed at 1111, 1059, 753, and 566 cm^{-1}, respectively. For the compound 9, the –C–O vibration signal was observed at 1023 cm^{-1}. For the compound 11, the asymmetric and symmetric stretching frequencies of nitro ($–NO_2$) group were observed at 1462 and 1293 cm^{-1}. These findings correspond well with the data reported in earlier research on analogous compounds (Al-Amiery et al., 2012; Tokalı et al., 2023b; Yakan et al., 2023a; Yakan, et al., 2023b). Table 3 provides an overview of the prominent IR stretching vibrations of the synthesized compounds.

^{1}H and ^{13}C NMR Analysis

The ^{1}H NMR spectra of the synthesized compounds were detected in DMSO-d_6 and the chemical shifts are given in Table 4. For compounds 4-11, the amino signal (-NH, H4) of thiosemicarbazone moiety was detected as a singlet in the ranges of 12.64 – 12.42 ppm, while the amino signal (–NH, H5) of isatin ring was observed as a singlet at 11.83 – 11.04 ppm, respectively. Also, the amino signal (–NH, H3) of the isopropyl region coupled to the methine group (>CH–) resonated as a doublet at 9.18 – 8.86 ppm. The methine group (>CH–, H2) of the isopropyl region was resonated as a multiplet (heptet) at 4.62 – 4.49 ppm; the methyl proton (CH_3, H1) signal was observed as a doublet at 1.30 – 1.28 ppm. The aromatic proton (H6-H8) signals of isatin ring were detected in the ranges of 8.63 – 6.80 ppm (see at Figures S9-S16 in Supplementary information). The methoxy ($–OCH_3$) proton signal of compound 9 was observed as a singlet at 3.78 ppm. The methyl ($–CH_3$) proton signal of compound 10 was observed as a singlet at 2.31 ppm. The results obtained are in good agreement with those documented in the literature for similar compounds (Al-Amiery et al., 2012; Yakan et al., 2023a; Yakan et al., 2023b). DMSO-d_6 and water in DMSO (HOD, H_2O) signals were seen around at 2.50 (quintet) and 3.30 (variable, based on the solvent and its concentration) ppm, respectively (Fleming & Williams, 2020).

The ^{13}C NMR spectra of the synthesized compounds were detected in DMSO-d_6 and the chemical shifts are presented in Table 5. For compounds 4–11, the characteristic –C=S peaks of the thiosemicarbazone moiety were detected at 176.26 – 176.16 ppm. The characteristic –C=O peaks of the isatin ring were detected at 163.48 – 162.51 ppm. The other characteristic –C=N (imine) peaks were observed in the ranges 143.15 – 136.42 ppm. The methine (>CH–, C2) carbon signal of the isopropyl region was detected 47.37 – 47.11 ppm; the methyl proton (CH_3, C1) signal was observed at 22.02 – 21.95 ppm. The aromatic carbon atom (C3-C8) signals of isatin ring were observed in the ranges of 159.89 – 85.75 ppm (see at Figures S17-S24 in Supplementary information). For all compounds, certain carbon atom signals in the range of 159.89 to 130.00 ppm were observed to be downfield (higher δ values) compared to the signal of the phenyl carbon at 128.5 ppm. This shift is attributed to the presence of substituent groups such as methoxy (–OCH_3), methyl (–CH_3), –F, –Cl, –NO_2, –Br, and –I. In compound 9, the methoxy carbon signal appeared at 56.24 ppm, while in compound 10, the methyl carbon signal was detected at 21.06 ppm. These observations are consistent with findings reported in previous studies on similar compounds (Al-Amiery et al., 2012; Yakan et al., 2023a; Yakan et al., 2023b; Altunoluk et al., 2024).

Table 4. Experimental and Theoretical ^1H NMR Data of the Synthesized Compounds, (δ/ppm)

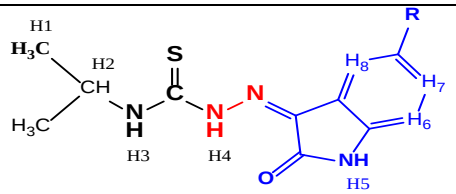

	Comp.	H1	H2	H3, NH	H4, NH	H5, NH	H6-H8
Experimental	4	1.28 (d, *J* = 6.6 Hz, 6H)	4.59 – 4.50 (m, 1H)	8.88 (d, *J* = 8.3 Hz, 1H)	12.58 (s, 1H)	11.22 (s, 1H)	7.73 (d, *J* = 7.5 Hz, 1H), 7.36 (t, *J* = 7.7 Hz, 1H), 7.11 (t, *J* = 7.6 Hz, 1H), 6.94 (d, *J* = 7.8 Hz, 1H)
	5	1.28 (d, *J* = 6.6 Hz, 6H)	4.58 – 4.50 (m, 1H)	8.90 (d, *J* = 8.4 Hz, 1H)	12.48 (s, 1H)	11.22 (s, 1H)	7.60 (dd, *J* = 8.1, 2.6 Hz, 1H), 7.19 (td, *J* = 8.7, 2.7 Hz, 1H), 6.92 (dd, *J* = 8.6, 4.1 Hz, 1H)
	6	1.28 (d, *J* = 6.6 Hz, 6H)	4.55 – 4.50 (m, 1H)	8.95 (d, *J* = 8.5 Hz, 1H)	12.44 (s, 1H)	11.31 (s, 1H)	7.83 (d, *J* = 2.2 Hz, 1H), 7.38 (dd, *J* = 8.4, 2.2 Hz, 1H), 6.94 (d, *J* = 8.3 Hz, 1H)
	7	1.28 (d, *J* = 6.5 Hz, 6H)	4.61 – 4.49 (m, 1H)	8.97 (d, *J* = 8.4 Hz, 1H)	12.44 (s, 1H)	11.32 (s, 1H)	7.95 (s, 1H), 7.51 (d, *J* = 7.9 Hz, 1H), 6.89 (d, *J* = 8.3 Hz, 1H)
	8	1.28 (d, *J* = 6.6 Hz, 6H)	4.59 – 4.50 (m, 1H)	8.98 (d, *J* = 8.5 Hz, 1H)	12.47 (s, 1H)	11.40 (s, 1H)	8.08 (d, *J* = 1.7 Hz, 1H), 7.66 (dd, *J* = 8.2, 1.8 Hz, 1H), 6.80 (d, *J* = 8.2 Hz, 1H)
	9	1.28 (d, *J* = 6.6 Hz, 6H)	4.60 – 4.49 (m, 1H)	8.86 (d, *J* = 8.3 Hz, 1H)	12.64 (s, 1H)	11.04 (s, 1H)	7.34 (s, 1H), 6.95 (d, *J* = 12.3 Hz, 1H), 6.85 (d, *J* = 8.5 Hz, 1H) OCH_3: 3.78 (s, 3H)
	10	1.28 (d, *J* = 6.6 Hz, 6H)	4.61 – 4.49 (m, 1H)	8.84 (d, *J* = 8.5 Hz, 1H)	12.58 (s, 1H)	11.10 (s, 1H)	7.54 (s, 1H), 7.15 (d, *J* = 7.9 Hz, 1H), 6.80 (d, *J* = 7.9 Hz, 1H) CH_3: 2.31 (s, 3H)
	11	1.30 (d, *J* = 6.6 Hz, 6H)	4.62 – 4.52 (m, 1H)	9.18 (d, *J* = 8.4 Hz, 1H)	12.42 (s, 1H)	11.83 (s, 1H)	8.63 (s, 1H), 8.27 (d, *J* = 8.7 Hz, 1H), 7.12 (d, *J* = 8.7 Hz, 1H)
Calculated	4	1.03-1.70	4.71	8.03	13.05	7.78	7.55-8.11
	5	1.03-1.70	4.71	8.04	13.02	7.77	7.29-7.80
	6	1.04-1.69	4.72	8.06	12.99	7.81	7.30-8.05
	7	1.04-1.69	4.72	8.05	12.99	7.80	7.29-8.09
	8	1.03-1.70	4.71	8.04	12.97	7.78	7.28-8.18
	9	1.05-1.65	4.74	8.04	13.00	7.60	7.23-7.58
	10	1.04-1.66	4.74	8.02	13.00	7.70	7.19-7.97
	11	1.07-1.69	4.74	8.16	12.83	8.18	7.45-911

Table 5. Experimental and Theoretical ^{13}C NMR Data of the Synthesized Compounds, (δ/ppm)

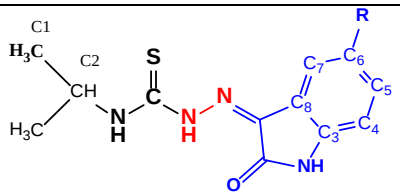

	Comp.	C1	C2	C=S	C=N	C=O	C3	C4	C5	C6	C7	C8
Experimental	4	22.00	47.13	176.26	142.71	163.11	132.19	120.41	131.62	121.61	122.68	111.49
	5	22.01	47.16	176.22	138.95	163.21	131.62, 131.59	112.57, 112.49	117.92, 117.68	159.89 157.53	108.70, 108.45	121.91, 121.82
	6	22.01	47.18	176.19	141.34	162.90	131.01	121.16	130.82	126.94	122.33	112.96
	7	22.01	47.19	176.18	141.73	162.77	133.61	113.43	130.89	114.57	123.91	122.73
	8	22.01	47.20	176.18	142.21	162.51	130.78	122.94	139.38	85.75	129.42	113.86
	9	22.02	47.17	176.24	136.42	163.27	132.52	121.24	112.19	155.76 OCH_3: 56.24	117.42	107.23
	10	22.01	47.11	176.24	140.48	163.19	132.31	120.42	131.75	132.03 CH_3: 21.06	121.86	111.22
	11	21.95	47.37	176.16	143.15	163.48	130.31	116.93	127.32	147.76	121.42	111.64
Calculated	4	21.99	52.34	184.77	136.56	169.17	149.28	115.87	137.91	128.36	126.00	126.68
	5	21.95, 21.91	52.47	184.87	135.80	169.23	145.26	116.94	123.31	169.32	112.52	128.11
	6	21.97, 21.92	52.48	184.88	135.16	168.90	147.56	117.15	136.9	141.41	125.72	128.37
	7	21.96, 21.91	52.50	184.88	135.10	168.77	148.08	117.38	139.68	139.27	128.46	128.55
	8	21.97, 21.91	52.47	184.87	135.12	168.59	148.62	117.56	144.67	130.83	133.29	128.67
	9	22.05, 22.10	52.28	184.71	137.20	169.28	142.29	117.00	125.49	164.30 OCH_3: 57.39	106.08	127.18
	10	22.10, 22.04	52.27	184.67	136.92	169.25	146.54	115.14	138.02	141.30 CH_3: 21.97	126.32	127.02
	11	21.98, 21.87	52.70	184.95	133.34	169.44	155.37	116.02	135.07	149.83	122.55	127.61

DFT Analysis

The analyses revealed that all compounds (compounds 4–11) exhibit a similar distribution of HOMO and LUMO localization. It was observed that the HOMO localization of the compounds is concentrated particularly on the sulfur (S) atom and the hydrazine (-NH-N=) moiety of the thiosemicarbazone chain (Figure 2; see Figures 25-26 in Supplementary Materials for all compounds). ESP maps also indicate that the highest negative electrostatic potential is located on the sulfur atom and, to a very minor extent on the carbonyl group of the isatin ring (except for compound 9). These findings suggest that the electron-donating ability of the molecule originates from these regions, making them the most probable target site for electrophilic attacks. In contrast, the LUMO localization of the compounds was observed to be distributed over the isatin ring and thiosemicarbazone moiety system. ESP maps reveal that this region possesses a significant positive potential, indicating that the main targets for nucleophilic attacks are the isatin ring, especially the carbonyl carbon atoms within this ring.

In addition, considering the effect of substituents, electron-donating and electron-withdrawing groups have caused significant changes in the ESP: Due to the nitro ($-NO_2$) group in compound 11, a strong electron-withdrawing effect has occurred in this region and the adjacent aromatic ring, resulting in a positive shift in the potential surface in terms of electron density. This situation has also increased the overall electrophilicity of the compound. In contrast, the methoxy ($-OCH_3$) group present in compound 9 has partially reduced the positive potential of the molecule by increasing the electron density on the aromatic ring.

Substituent groups alter the electronic properties of compounds primarily through inductive and/or mesomeric (resonance) effects. In this context, electron-withdrawing groups (EWG) and electron-donating groups (EDG) lead to different chemical behaviours. Halogens (–F, –Cl, –Br, –I; compounds 5–8), which are classified among EWGs, withdraw electrons via inductive effects, while exhibiting weak electron-donating characteristics from a mesomeric perspective. Compared to the reference compound (compound 4), these groups lower both the HOMO and LUMO energy levels, thereby

stabilizing the molecule. The nitro group (–NO_2; compound 11), which is the strongest EWG in the series, acts as a very strong electron-withdrawing group through both inductive and mesomeric effects. This group causes the largest decrease in orbital energy levels among all substituents. This effect not only makes the molecule containing the nitro group more reactive toward chemical reactions but also enhances the electrophilic character of the compound.

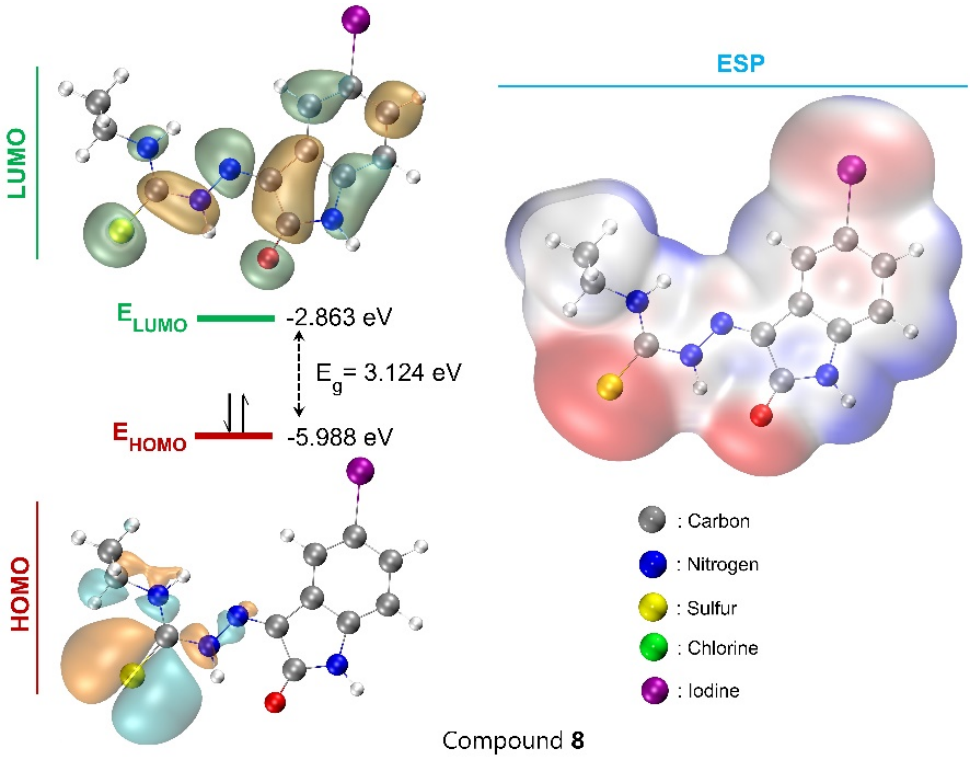

Figure 2. HOMO-LUMO and ESP Maps of Compound 8

Methyl group (-CH_3; compound 10), as an electron-donating group, slightly raises the HOMO and LUMO energy levels relative to the reference through its weak inductive and hyperconjugative effects. This effect enhances the molecule's reactivity and nucleophilicity. Methoxy group (-OCH_3; compound 9), although inductively electron-withdrawing, acts as a strong electron-donating group via its resonance (mesomeric) effect due to the lone pair of electrons on the oxygen atom. As a result of this dual effect, compound 9 exhibits the highest HOMO energy level in the series, making it potentially the best electron donor (nucleophile) among the compounds studied.

The effects of substituents on the FMO energy eigenvalues and global reactivity parameters of the compounds are given in Table 6. At this point, the -NO_2 substituted compound 11 stands out as the most reactive compound in the series, possessing the lowest energy gap (Eg = 3.016 eV) and hardness (η = 1.508 eV). On the other hand, the methyl-substituted compound 10 exhibits the highest energy gap of 3.211 eV, indicating that it is the most stable compound in the series. In this context, the reactivity order from highest to lowest can be given as: 11 > 8 ≈ 7 > 6 > 5 > 9 > 4 > 10.

The electronegativity (χ) and electrophilicity index (ω) parameters are related to a molecule's electron-withdrawing tendency and electron-accepting capacity. In this context, compound 11, with an electronegativity of 4.682 eV and an electrophilicity value of 7.269 eV, can be identified as the strongest electrophile in the series. Among the compounds with EDGs, compound 10 (-CH_3) and compound 9 (-OCH_3) have the lowest electrophilicity indices, with values of 5.591 eV and 5.668 eV, respectively. Accordingly, the electrophilicity ranking of the compounds is determined as 11 > 7 > 6 > 8 > 5 > 4 > 9 > 10, reflecting their potential to react with nucleophiles.

Finally, the nucleophilicity index (ε) and electrodonating power (ω^-) provide information about the electron-donating ability of molecule, which is enhanced by EDGs. Compound 9 ($-OCH_3$) and compound 10 ($-CH_3$) exhibited the highest nucleophilicity indices, with values of 3.669 eV and 3.652 eV, respectively. In contrast, compound 11 ($-NO_2$) showed the lowest nucleophilicity, with a value of 3.305 eV. A similar trend was observed in terms of electrodonating power (ω^-), where compound 6 (5.350 eV) and compound 10 (5.315 eV) were identified as the best electron donors.

Table 6. Calculated Electronic Parameters of the Compounds

Comp.	E_{HOMO} (eV)	E_{LUMO} (eV)	E_g (eV)	η (eV)	χ (eV)	ω (eV)	**ε** (eV)	ω^+ (eV)	ω^- (eV)
4	-5.873	-2.687	3.186	1.593	4.280	5.749	3.621	1.133	5.413
5	-5.979	-2.841	3.138	1.569	4.410	6.196	3.516	1.286	5.695
6	-5.998	-2.870	3.128	1.564	4.434	6.286	3.497	1.317	5.751
7	-6.002	-2.878	3.124	1.562	4.440	6.310	3.493	1.326	5.766
8	-5.988	-2.863	3.124	1.562	4.425	6.268	3.507	1.312	5.737
9	-5.826	-2.654	3.172	1.586	4.240	5.668	3.669	1.110	5.350
10	-5.842	-2.632	3.211	1.605	4.237	5.591	3.652	1.079	5.315
11	-6.190	-3.174	3.016	1.508	4.682	7.269	3.305	1.670	6.352

*E_g: $E_{LUMO} - E_{HOMO}$, η: Chemical Hardness, χ: Electronegativity, ω: Electrophilic index, **ε**: Nucleophilic index, ω+ : Electroaccepting power, ω- : Electrodonating power*

Conclusion

A new series of isatin-based isopropyl-thiosemicarbazone derivatives (4–11) was prepared successfully. The compounds were obtained in moderate to good yields, ranging from 60% to 95%. Their chemical structures were characterized using IR, ^{1}H and ^{13}C NMR spectroscopy, along with elemental analysis. The computational analyses have shown that both electron-withdrawing and electron-donating substituents influence the electronic structure, orbital distribution, and reactivity of isatin derivative thiosemicarbazones. The sulphur atom and the hydrazine group (thiosemicarbazone moiety) emerged as electrophilic interaction regions, while the isatin ring, particularly the carbonyl carbon, was identified as a nucleophilic target. Among the substituents, the nitro group provided the highest electrophilic character and the lowest energy gap, making compound 11 the most reactive compound in the series. In contrast, the methoxy group increased nucleophilicity and raised the HOMO level, identifying compound 9 as the best electron donor in the series. It has been demonstrated that structural and electronic properties of the compounds are modulated by inductive and mesomeric effects, and within this context, the dependence of electronegativity, electrophilicity, and nucleophilicity indices on these effects has been revealed.

Ethics

There are no ethical issues regarding the publication of this article.

Conflict of Interest

The author declares that he has no conflict of interest.

ORCID

Hakan Yakan http://orcid.org/0000-0002-4428-4696

References

Al-Amiery, A. A., Al-Majedy, Y. K., Ibrahim, H. H., & Al-Tamimi, A. A. (2012). Antioxidant, antimicrobial, and theoretical studies of the thiosemicarbazone derivative Schiff base 2-(2-imino-1-methylimidazolidin-4-ylidene) hydrazinecarbothioamide (IMHC). *Organic and medicinal chemistry letters*, *2*(4), 1-7. https://doi.org/10.1186/2191-2858-2-4

Altunoluk, O. C., Özbek, O., Kalay, E., Tokalı, F. S., & Aslan, O. N. (2024). Surface characterization of barium (II)-selective potentiometric sensor based on a newly synthesized thiosemicarbazone derivative molecule. *Electroanalysis*, *36*(7), e202300407. https://doi.org/10.1002/elan.202300407

Arafath, M. A. (2024). Thiosemicarbazone Schiff base ligands and their complexes with nickel, palladium and platinum show anticancer and antibacterial activities. *Journal of Sulfur Chemistry*, *45*(1), 138-171. https://doi.org/10.1080/17415993.2023.2255711

Bal, T. R., Anand, B., Yogeeswari, P., & Sriram, D. (2005). Synthesis and evaluation of anti-HIV activity of isatin β-thiosemicarbazone derivatives. *Bioorganic and Medicinal Chemistry Letters*, *15*(20), 4451-4455. https://doi.org/10.1016/j.bmcl.2005.07.046

Cramer, C. J. (2013). *Essentials of computational chemistry: theories and models*. John Wiley & Sons.

Czylkowska, A., Pitucha, M., Raducka, A., Fornal, E., Kordialik-Bogacka, E., Ścieszka, S., Smoluch, M., Burdan, F., Jędrzejec, M., & Szymański, P. (2024). Thiosemicarbazone-based compounds: A promising scaffold for developing antibacterial, antioxidant, and anticancer therapeutics. *Molecules*, *30*(1), 129. https://doi.org/10.3390/molecules30010129

Çavuş, M. S. (2025). Synthesis of new 5-iodoisatin derivatives: Predicting antioxidant inhibition activity with DFT studies. *Journal of Molecular Structure*, *1323*, 140826. https://doi.org/10.1016/j.molstruc.2024.140826

Deng, X. Q., & Song, M. X. (2014). Design and synthesis of pyrazolyl thiosemicarbazones as new anticonvulsants. *Bulletin of the Korean Chemical Society*, *35*(9), 2733-2737. https://doi.org/10.5012/bkcs.2014.35.9.2733

Fleming, I., & Williams, D. (2020). *Spectroscopic methods in organic chemistry* (Seventh Edition ed.). Springer Nature. https://doi.org/10.1007/978-3-030-18252-6

Govender, H., Mocktar, C., Kumalo, H. M., & Koorbanally, N. A. (2019). Synthesis, antibacterial activity and docking studies of substituted quinolone thiosemicarbazones. *Phosphorus, Sulfur, and Silicon and the Related Elements*, *194*(11), 1074-1081. https://doi.org/10.1080/10426507.2019.1618298

Gündüz, M. G., Kaya, B., Özkul, C., Şahin, O., Rekha, E. M., Sriram, D., & Ülküseven, B. (2021). S-alkylated thiosemicarbazone derivatives: Synthesis, crystal structure determination, antimicrobial activity evaluation and molecular docking studies. *Journal of Molecular Structure*, *1242*, 130674. https://doi.org/10.1016/j.molstruc.2021.130674

Hall, M. D., Brimacombe, K. R., Varonka, M. S., Pluchino, K. M., Monda, J. K., Li, J., Walsh, M. J., Boxer, M. B., Warren, T. H., & Fales, H. M. (2011). Synthesis and structure–activity evaluation of isatin-β-thiosemicarbazones with improved selective activity toward multidrug-resistant cells expressing P-glycoprotein. *Journal of Medicinal Chemistry*, *54*(16), 5878-5889. https://doi.org/10.1021/jm2006047

Hameed, A., Khan, K. M., Zehra, S. T., Ahmed, R., Shafiq, Z., Bakht, S. M., Yaqub, M., Hussain, M., de León, A. d. l. V., & Furtmann, N. (2015). Synthesis, biological evaluation and molecular docking of N-phenyl thiosemicarbazones as urease inhibitors. *Bioorganic Chemistry*, *61*, 51-57. https://doi.org/10.1016/j.bioorg.2015.06.004

Hernández, W., Carrasco, F., Vaisberg, A., Spodine, E., Icker, M., Krautscheid, H., Beyer, L., Tamariz-Angeles, C., & Olivera-Gonzales, P. (2023). Novel thiosemicarbazone derivatives from furan-2-carbaldehyde: synthesis, characterization, crystal structures, and antibacterial, antifungal, antioxidant, and antitumor activities. *Journal of chemistry*, *2023*, 1-20. https://doi.org/10.1155/2023/5413236

Hohenberg, P., & Kohn, W. (1964). Inhomogeneous Electron Gas. *Physical Review*, *136*(3B), B864-B871. https://doi.org/10.1103/PhysRev.136.B864

Islam, M., Khan, A., Shehzad, M. T., Hameed, A., Ahmed, N., Halim, S. A., Khiat, M., Anwar, M. U., Hussain, J., & Csuk, R. (2019). Synthesis and characterization of new thiosemicarbazones, as potent urease inhibitors: In vitro and in silico studies. *Bioorganic Chemistry*, *87*, 155-162. https://doi.org/10.1016/j.bioorg.2019.03.008

Karakuş, F. G., Tunalı, S., Bal-demirci, T., Ülküseven, B., & Yanardağ, R. (2024). Ameliorative Effect of a Vanadium-thiosemicarbazone Complex on Oxidative Stress in Stomach Tissue of Experimental Diabetic Rats. *Sakarya University Journal of Science*, *28*(1), 133-144. https://doi.org/10.16984/saufenbilder.1289079

Koch, W., & Holthausen, M. C. (2015). *A chemist's guide to density functional theory*. John Wiley & Sons.

Kohn, W., Becke, A. D., & Parr, R. G. (1996). Density functional theory of electronic structure. *Journal of Physical Chemistry*, *100*(31), 12974-12980. https://doi.org/10.1021/jp960669l

Kohn, W., & Sham, L. J. (1965). Self-consistent equations including exchange and correlation effects. *Physical review*, *140*(4A), A1133-A1138. https://doi.org/10.1103/PhysRev.140.A1133

Kshirsagar, A., Toraskar, M. P., Kulkarni, V. M., Dhanashire, S., & Kadam, V. (2009). Microwave assisted synthesis of potential anti infective and anticonvulsant thiosemicarbazones. *International Journal of ChemTech Research*, *1*(3), 696-701.

Muğlu, H. (2020). Synthesis, characterization, and antioxidant activity of some new N 4-arylsubstituted-5-methoxyisatin-β-thiosemicarbazone derivatives. *Research on Chemical Intermediates*, *46*(4), 2083-2098. https://doi.org/10.1007/s11164-020-04079-x

Neese, F. (2022). Software update: The ORCA program system—Version 5.0. *Wiley Interdisciplinary Reviews: Computational Molecular Science*, *12*(5), e1606. https://doi.org/10.1002/wcms.1606

Ozcan, E., Vagolu, S. K., Gunduz, M. G., Stevanovic, M., Kokbudak, Z., Tønjum, T., Nikodinovic-Runic, J., Çetinkaya, Y., & Dogan, S. D. (2023). Novel quinoline-based thiosemicarbazide derivatives: synthesis, DFT calculations, and investigation of antitubercular, antibacterial, and antifungal activities. *ACS omega*, *8*(43), 40140-40152. https://doi.org/10.1021/acsomega.3c03018

Parr, R. G. (1989). Density functional theory of atoms and molecules. Horizons of Quantum Chemistry: Proceedings of the Third International Congress of Quantum Chemistry Held at Kyoto, Japan, October 29-November 3, 1979.

Parr, R. G., & Yang, W. (1984). Density functional approach to the frontier-electron theory of chemical reactivity. *Journal of the American Chemical Society*, *106*(14), 4049-4050. https://doi.org/10.1021/ja00326a036

Pervez, H., Iqbal, M. S., Tahir, M. Y., Nasim, F.-u.-H., Choudhary, M. I., & Khan, K. M. (2008). In vitro cytotoxic, antibacterial, antifungal and urease inhibitory activities of some N 4-substituted isatin-3-thiosemicarbazones. *Journal of Enzyme Inhibition and Medicinal Chemistry*, *23*(6), 848-854. https://doi.org/10.1080/14756360701746179

Sevinçli, Z. Ş., Duran, G. N., Özbil, M., & Karalı, N. (2020). Synthesis, molecular modeling and antiviral activity of novel 5-fluoro-1H-indole-2, 3-dione 3-thiosemicarbazones. *Bioorganic Chemistry*, *104*, 104202. https://doi.org/10.1016/j.bioorg.2020.104202

Shakya, B., & Yadav, P. N. (2020). Thiosemicarbazones as potent anticancer agents and their modes of action. *Mini Reviews in Medicinal Chemistry*, *20*(8), 638-661. https://doi.org/10.2174/1389557519666191029130310

Shehzad, M. T., Khan, A., Islam, M., Hameed, A., Khiat, M., Halim, S. A., Anwar, M. U., Shah, S. R., Hussain, J., & Csuk, R. (2020). Synthesis and urease inhibitory activity of 1, 4-benzodioxane-based thiosemicarbazones: Biochemical and computational approach. *Journal of Molecular Structure*, *1209*, 127922. https://doi.org/10.1016/j.molstruc.2020.127922

Subhashree, G., Haribabu, J., Saranya, S., Yuvaraj, P., Krishnan, D. A., Karvembu, R., & Gayathri, D. (2017). In vitro antioxidant, antiinflammatory and in silico molecular docking studies of thiosemicarbazones. *Journal of Molecular Structure*, *1145*, 160-169. https://doi.org/10.1016/j.molstruc.2017.05.054

Tokalı, F. S., Şenol, H., Katmerlikaya, T. G., Dağ, A., & Şendil, K. (2023a). Novel thiosemicarbazone and thiazolidin-4-one derivatives containing vanillin core: Synthesis, characterization, and anticancer activity studies. *Journal of Heterocyclic Chemistry*, *60*(4), 645-656. https://doi.org/10.1002/jhet.4619

Tokalı, F. S., Taslimi, P., Tüzün, B., Karakuş, A., Sadeghian, N., & Gulçin, İ. (2023b). Synthesis of new carboxylates and sulfonates containing thiazolidin-4-one ring and evaluation of inhibitory properties against some metabolic enzymes. *Journal of the Iranian Chemical Society*, *20*(10), 2631-2642. https://doi.org/10.1007/s13738-023-02861-3

Tokalı, F. S., Taslimi, P., Usanmaz, H., Karaman, M., & Şendil, K. (2021). Synthesis, characterization, biological activity and molecular docking studies of novel schiff bases derived from thiosemicarbazide: Biochemical and computational approach. *Journal of Molecular Structure*, *1231*, 129666. https://doi.org/10.1016/j.molstruc.2020.129666

Yakan, H. (2020). Preparation, structure elucidation, and antioxidant activity of new bis (thiosemicarbazone) derivatives. *Turkish Journal of Chemistry*, *44*(4), 1085-1099. https://doi.org/10.3906/kim-2002-76

Yakan, H., Azam, M., Kansız, S., Muğlu, H., Ergül, M., Taslimi, P., Koçyiğit, Ü. M., Karaman, M., Al-Resayes, S. I., & Min, K. (2023a). Isatin/thiosemicarbohydrazone hybrids: Facile synthesis, and their evaluation as anti-proliferatıve agents and metabolıc enzyme inhibitors. *Bulletin of the Chemical Society of Ethiopia*, *37*(5), 1221-1236. https://doi.org/10.4314/bcse.v37i5.14

Yakan, H., Muğlu, H., Türkeş, C., Demir, Y., Erdoğan, M., Çavuş, M. S., & Beydemir, Ş. (2023b). A novel series of thiosemicarbazone hybrid scaffolds: Design, synthesis, DFT studies, metabolic enzyme inhibition properties, and molecular docking calculations. *Journal of Molecular Structure*, *1280*, 135077. https://doi.org/10.1016/j.molstruc.2023.135077

Zhang, Y.-M., Wang, D.-D., Lin, Q., & Wei, T.-B. (2007). Synthesis and anion recognition properties of thiosemicarbazone based molecular tweezers. *Phosphorus, Sulfur, and Silicon and the Related Elements*, *183*(1), 44-55. https://doi.org/10.1080/10426500701555777